UNCLASSIFIED

AD 404 858

DEFENSE DOCUMENTATION CENTER

FOR

SCIENTIFIC AND TECHNICAL INFORMATION

CAMERON STATION, ALEXANDRIA, VIRGINIA

UNCLASSIFIED

NOTICE: When government or other drawings, specifications or other data are used for any purpose other than in connection with a definitely related government procurement operation, the U. S. Government thereby incurs no responsibility, nor any obligation whatsoever; and the fact that the Government may have formulated, furnished, or in any way supplied the said drawings, specifications, or other data is not to be regarded by implication or otherwise as in any manner licensing the holder or any other person or corporation, or conveying any rights or permission to manufacture, use or sell any patented invention that may in any way be related thereto.

63 3 5

D1-82-0230

404 858

CATALOGED BY ASTIA
AS AD No. 404858

BOEING SCIENTIFIC RESEARCH LABORATORIES

Slender Bodies of Revolution Having Minimum Total Drag at Hypersonic Speeds

Angelo Miele
David G. Hull

MAY 28 1963

February 1963

D1-82-0230

BOEING SCIENTIFIC RESEARCH LABORATORIES

FLIGHT SCIENCES LABORATORY TECHNICAL REPORT NO. 70

SLENDER BODIES OF REVOLUTION HAVING MINIMUM TOTAL DRAG AT HYPERSONIC SPEEDS

ANGELO MIELE and DAVID G. HULL

FEBRUARY 1963

TABLE OF CONTENTS

SLENDER BODIES OF REVOLUTION HAVING MINIMUM TOTAL DRAG AT HYPERSONIC SPEEDS

by

ANGELO MIELE(*) and DAVID G. HULL(**)

SUMMARY

This paper considers the problem of minimizing the total drag (sum of the pressure drag and the friction drag) of a slender, axisymmetric body at zero angle of attack in hypersonic flow under the assumption that the distribution of pressure coefficients is Newtonian and that the friction coefficient is constant. After the condition that the pressure coefficient be nonnegative is accounted for, the minimal problem is solved for arbitrary conditions imposed on the diameter, the length, and the volume under the assumption that the wetted area is free. It is shown that, if convenient dimensionless coordinates are employed (that is, if the abscissa and the ordinate are normalized with respect to the length and the semithickness), the totality of extremal arcs is composed of a two-parameter family of solutions. Each extremal arc involves at most two corner points and, hence, three subarcs: one of these is characterized by a positive pressure coefficient and is called the regular shape; the other two are characterized by a zero pressure coefficient and are called the zero-slope shapes. Thus, four classes of bodies can be identified: (I) bodies com-

---

(*)Director of Astrodynamics and Flight Mechanics, Boeing Scientific Research Laboratories.

(**)Staff Associate, Boeing Scientific Research Laboratories.

posed of a regular shape only, (II) bodies composed of a spike followed by a regular shape, (III) bodies composed of a regular shape followed by a cylinder, and (IV) bodies composed of a spike followed by a regular shape followed by a cylinder.

Particular attention is devoted to solutions for which one, two, or three of the quantities under consideration are prescribed. If only one quantity is given (the diameter or the volume), the extremal arc consists of a single subarc of class I regardless of the friction coefficient. If two geometric quantities are given (the diameter and the length, the diameter and the volume, or the length and the volume), a one-parameter family of extremal arcs exists which involves at most two subarcs; the associated parameter, called the friction parameter, is proportional to the cubic root of the friction coefficient and is related to the quantities which are prescribed. Finally, if three geometric quantities are given (the diameter, the length, and the volume), a two-parameter family of extremal arcs exists which involve at most three subarcs; these parameters, called the friction and the shape parameters, are related to the friction coefficient and the geometric quantities which are prescribed. For each of the cases considered, analytical expressions are derived for the optimum shape, the thickness ratio, and the drag coefficient.

1. INTRODUCTION

The problem of minimizing the drag of slender bodies of revolution in hypersonic flow has attracted considerable attention in recent times. With particular regard to the pressure drag, generalized solutions have been obtained in Ref. 1 under the assumption that the pressure distribution is Newtonian and that, among the geometrical quantities being considered (the diameter, the length, the wetted area, and the volume), two are prescribed and the remaining two are free. These solutions have been extended in Ref. 2 to cover the case where three of these quantities are given and only one is free.

While the investigations of Refs. 1 and 2 neglected the friction drag, it should be noted that there exist practical values of the thickness ratio for which the friction drag may have the same order of magnitude as the pressure drag. Therefore, it is of interest to reinvestigate the problem of the optimum slender shape from the point of view of minimizing the total forebody drag, that is, the sum of the pressure drag and the friction drag.

For the case where the diameter and the length are prescribed, previous investigations were carried out by Kennet (Ref. 3) assuming that the friction coefficient is constant and by Miele and Cole (Ref. 4) assuming that the distribution of friction coefficients along the contour is represented by a power law. A more general problem consists of minimizing the total drag for any number of conditions imposed on the diameter d, the length ℓ, the wetted area S, and the volume V. This is the problem considered in the present report in connection with the following assumptions: (a) the body is slender and has a circular cross-section; (b) the distribution of pressure coefficents

is Newtonian; and (c) the friction coefficient is constant along the contour. The corresponding two-dimensional problem is analyzed in Ref. 5 for any number of conditions imposed on the thickness, the length, the enclosed area, and the moment of inertia of the contour.

2. MINIMUM DRAG PROBLEM

Consider a body of revolution at zero angle of attack in a hypersonic flow, and denote by x an axial coordinate, y a radial coordinate, and $\dot{y}$ the derivative dy/dx. Under the slender body approximation $\dot{y}^2 \ll 1$, the assumed Newtonian distribution of pressure coefficients simplifies to $C_p = 2\dot{y}^2$. Consequently, the drag of that portion of the body which is included between stations 0 and x is given by

$$D(x) = 4\pi q \int_0^x y\left(\dot{y}^3 + \frac{C_f}{2}\right) dx \tag{1}$$

where C_f is the friction coefficient, assumed constant. The corresponding values of the wetted area and the volume are given by

$$S(x) = 2\pi \int_0^x y\, dx\,, \qquad V(x) = \pi \int_0^x y^2\, dx \tag{2}$$

After the definitions

$$\alpha = \frac{D(x)}{4\pi q}\,, \qquad \beta = \frac{S(x)}{2\pi}\,, \qquad \alpha = \frac{V(x)}{\pi} \tag{3}$$

are introduced, differentiation of both sides of Eqs. (1) and (2) with respect to the independent variable leads to the following differential constraints:

$$\dot{\alpha} - y\left(\dot{y}^3 + \frac{C_f}{2}\right) = 0$$

$$\dot{\beta} - y = 0 \tag{4}$$

$$\dot{\gamma} - y^2 = 0$$

Since the requirement that the slope be nonnegative everywhere can be expressed as

$$\dot{y} - p^2 = 0 \tag{5}$$

where p denotes a real variable, the differential system composed of Eqs. (4) and (5) involves one independent variable (x), five dependent variables (y, α, β, γ, p), and one degree of freedom. In this connection, after assuming that

$$x_i = y_i = \alpha_i = \beta_i = \gamma_i = 0 \tag{6}$$

and that some, but not all, of the remaining state variables are given at the final point, one can formulate the minimum drag problem as follows: <u>In the class of functions $y(x)$, $\alpha(x)$, $\beta(x)$, $\gamma(x)$, $p(x)$ which are consistent with the differential constraints (4) and (5) and the initial conditions (6), find that special set which minimizes the difference $\Delta G = G_f - G_i$, where $G = \alpha$.</u>

3. NECESSARY CONDITIONS

The previous problem is of the Mayer type with separated end conditions. Consequently, after the Lagrange multipliers λ_1 through λ_4 are introduced and the fundamental function is written as (Refs. 6 and 7)

$$F = \lambda_1 \left[\dot{\alpha} - y\left(\dot{y}^3 + \frac{C_f}{2}\right) \right] + \lambda_2(\dot{\beta} - y) + \lambda_3(\dot{\gamma} - y^2) + \lambda_4(\dot{y} - p^2) \tag{7}$$

the extremal arc is described by the following Euler-Lagrange equations:

$$\begin{aligned} \frac{d}{dx}(\lambda_4 - 3\lambda_1 y\dot{y}^2) &= -\lambda_1\left(\dot{y}^3 + \frac{C_f}{2}\right) - \lambda_2 - 2\lambda_3 y \\ \dot{\lambda}_1 &= 0 \\ \dot{\lambda}_2 &= 0 \\ \dot{\lambda}_3 &= 0 \\ 0 &= \lambda_4 p \end{aligned} \tag{8}$$

the second, third, and fourth of which can be integrated to give

$$\lambda_1 = C_1 , \quad \lambda_2 = C_2 , \quad \lambda_3 = C_3 \tag{9}$$

where C_1, C_2, and C_3 are constants. Furthermore, after it is observed that the fundamental function does not contain the independent variable explicitly and after Eq. (8-5) is accounted for, the following first integral can be established:

$$C_1 y\left(\frac{C_f}{2} - 2\dot{y}^3\right) + C_2 y + C_3 y^2 = C \tag{10}$$

where C is a constant.

Corner conditions. As the fifth Euler equation indicates, the extremal arc is composed of the subarcs

$$\lambda_4 = 0 \text{ and/or } p = 0 \tag{11}$$

Along the former subarcs, called regular shapes, the pressure coefficient is always positive as long as p is real. Along the latter subarcs, called zero-slope shapes, the pressure coefficient is always zero. The junction between the subarcs must be studied with the aid of the Erdmann-Weierstrass corner conditions. They require that each of the integration constants C_1, C_2, C_3, C has the same value for all the subarcs composing the extremal arc and that(*)

$$\Delta(y\dot{y}^3) = \Delta(\lambda_4 - 3C_1 y\dot{y}^2) = 0 \tag{12}$$

where $\Delta(\ldots)$ denotes the difference between quantities evaluated after the corner and before the corner. These equations admit two sets of solutions

$$\begin{aligned} &y > 0 , \quad \Delta\lambda_4 = 0 , \quad \Delta\dot{y} = 0 \\ &y = 0 , \quad \Delta\lambda_4 = 0 \end{aligned} \tag{13}$$

(*) Eq. (12-1) is a consequence of the first integral (10) and the continuity of the integration constants.

meaning that the transition from one subarc to another occurs without a discontinuity in the slope away from the axis of symmetry but may occur with a discontinuity in the slope on the axis of symmetry. If Eqs. (11) and (13) are combined, the following relations can be shown to hold on both sides of a corner point:

$$\begin{aligned} y > 0 \;, \quad \lambda_4 = 0 \;, \quad \dot{y} = 0 \\ y = 0 \;, \quad \lambda_4 = 0 \end{aligned} \tag{14}$$

End conditions. The end conditions are partly of the fixed end-point type and partly of the natural type. The latter must be determined from the transversality condition

$$\left[- C\, dx + (C_1 + 1)\, d\alpha + C_2 d\beta + C_3 d\gamma + (\lambda_4 - 3C_1 y\dot{y}^2) dy \right]_i^f = 0 \tag{15}$$

which must be satisfied for every system of differentials consistent with the prescribed end conditions; in particular, it implies that $C_1 = -1$.

If the length is free, the transversality condition yields $C = 0$. On the other hand, if either the wetted area or the volume is free, the transversality condition leads to $C_2 = 0$ or $C_3 = 0$, respectively. Finally, if the diameter is free, the transversality condition leads to

$$(\lambda_4 + 3y\dot{y}^2)_f = 0 \tag{16}$$

which, if combined with the Euler-Lagrange equation (8-5), implies that

$$\lambda_{4f} = \dot{y}_f = 0 \tag{17}$$

Consequently, if $d = 2y_f$ denotes the diameter, the first integral (10) yields the additional relationship

$$C + C_f \frac{d}{4} - C_2 \frac{d}{2} - C_3 \frac{d^2}{4} = 0 \tag{18}$$

At this point, it is convenient to separate the discussion into two basic problems: problems where the wetted area is given and problems where the wetted area is free. As Eqs. (1) and (2-1) show, problems of the first kind are characterized by the fact that the friction drag is independent of the shape so that the contour which minimizes the total drag is identical with that which minimizes the pressure drag. Since shapes of minimum pressure drag have been fully discussed in Refs. 1 and 2, these problems are not considered here. Thus, the analysis is restricted to problems of the second kind, in which the wetted area is free. This class of problems contains several subclasses which depend on the number of quantities that are specified (one, two, or three). For these problems, simple manipulations lead to the results which are summarized in Table 1 where two types of relations are indicated: those obtained from the transversality condition and those obtained by combining the results of the transversality condition with the Euler-Lagrange equation (8-5) and the first integral (10).

Legendre-Clebsch condition. The Legendre-Clebsch condition indicates that the drag is a minimum if the following inequalities are satisfied every-

where along the extremal arc:

$$\begin{aligned} \dot{y} &\geq 0 , \quad \text{along the regular shape} \\ \lambda_4 &\leq 0 , \quad \text{along the zero-slope shape} \end{aligned} \tag{19}$$

Switching function. From the previous discussion, it appears that the Lagrange multiplier λ_4 plays an important role in determining the composition of the extremal arc. If the terminology of control theory is employed, this multiplier can be called the switching function; its properties are as follows:

$$\begin{aligned} \lambda_4 &= 0 , \quad \text{along the regular shape} \\ \lambda_4 &\leq 0 , \quad \text{along the zero-slope shape} \\ \lambda_4 &= 0 , \quad \text{at a corner point} \end{aligned} \tag{20}$$

4. GEOMETRY OF THE EXTREMAL ARC

In the previous section, the necessary conditions to be satisfied by the extremal arc have been stated. In this section, several general consequences of these equations are derived, referring, for the sake of brevity, to the minimum drag problem ($C_1 = -1$) with the wetted area unspecified ($C_2 = 0$). In order to facilitate the analysis, the following dimensionless coordinates are introduced:

$$\xi = x/\ell \ , \quad \eta = 2y/d \tag{21}$$

together with the definitions

$$K_1 = 4C/dC_f \ , \quad K_3 = C_3 d/C_f \tag{22}$$

With these coordinates, the first integral (10) reduces to the form

$$\frac{\tau^3}{2C_f}\,\eta\dot{\eta}^3 = K_1 + \eta - K_3\eta^2 \tag{23}$$

where $\tau = d/\ell$ denotes the thickness ratio and $\dot{\eta}$ the derivative $d\eta/d\xi$.

Basic inequalities. The application of the first integral at the end points of the extremal arc indicates that the terminal values of the slope are given by

$$(\sqrt[3]{\pi}\,\dot{\eta})_1 = \frac{\sqrt[3]{2C_f}}{\tau} K_1^{1/3}$$

$$\eta_f = \frac{\sqrt[3]{2C_f}}{\tau} (K_1 + 1 - K_3)^{1/3} \tag{24}$$

and, consequently, are nonnegative providing the following basic inequalities are satisfied:

$$K_1 \geq 0 , \quad K_1 + 1 - K_3 \geq 0 \tag{25}$$

Incidentally, the optimum shape is blunt-nosed if $K_1 > 0$ while it may be sharp-nosed if $K_1 = 0$.

Switching function. Since each extremal arc may involve more than one subarc, it is of paramount importance to calculate the distribution of the switching function; in nondimensional form, this function can be defined as

$$\sigma = \frac{2}{\ell C_f} \lambda_4 \tag{26}$$

For the regular shape, it is known that $\sigma = 0$. For the zero-slope shape, it is known that $\dot{\eta} = 0$ and $\eta = \text{const}$. Consequently, the Euler-Lagrange equation (8-1) reduces to

$$\dot{\sigma} = 1 - 2K_3\eta \tag{27}$$

which, in the light of the end condition (20-3), admits the particular integral

$$\sigma = (1 - 2K_3\eta_c)(\xi - \xi_c) \tag{28}$$

in which the subscript c refers to a corner point.

Sequence of subarcs. In order to determine the appropriate sequence of subarcs, it is necessary to decide: (a) whether a corner point between a regular shape and a zero-slope shape can occur; and (b) what the maximum number of corner points is. Concerning the first question, the corner conditions (14) and the first integral (23) show that the transition from a regular shape to a zero-slope shape, and vice versa, is possible if the following relationship is satisfied:

$$K_1 + \eta_c - K_3\eta_c^2 = 0 \tag{29}$$

With regard to the second question, Eq. (28) shows that, since the switching function varies linearly with the abscissa along the zero-slope shape, it can only vanish at one point of each zero-slope shape. Due to Eq. (20-3), this point must be the corner point between the regular shape and the zero-slope shape. This means that (a) the regular shape may be preceded or followed by no more than one zero-slope shape and (b) the equations of the zero-slope shapes can only be $\eta = 0$ and/or $\eta = 1$. Furthermore, because of Eq. (29) and the properties of the switching function, the presence of zero-slope shapes requires that

$$\eta = 0 \begin{cases} K_1 = 0 \end{cases}$$

$$\eta = 1 \begin{cases} K_1 + 1 - K_3 = 0 \\ 1 - 2K_3 \leq 0 \end{cases} \tag{30}$$

Since no more than two corner points and three subarcs can exist, the totality of extremal arcs consists of four classes of bodies: (I) bodies composed of a regular shape only, (II) bodies composed of a spike followed by a regular shape, (III) bodies composed of a regular shape followed by a cylinder, and (IV) bodies composed of a spike followed by a regular shape followed by a cylinder. These bodies are represented symbolically by

$$\begin{aligned} &\text{Class I:} && \sigma = 0 \\ &\text{Class II:} && \eta = 0 \rightarrow \sigma = 0 \\ &\text{Class III:} && \sigma = 0 \rightarrow \eta = 1 \\ &\text{Class IV:} && \eta = 0 \rightarrow \sigma = 0 \rightarrow \eta = 1 \end{aligned} \tag{31}$$

Family of solutions. Since the most general type of extremal arc is of class IV, its geometry can be described by the equations

$$\begin{aligned} &0 \leq \xi \leq \xi_0 , && \eta = 0 \\ &\xi_0 \leq \xi \leq \xi_1 , && \frac{\xi - \xi_0}{\xi_1 - \xi_0} = \frac{\int_0^{\eta} \eta^{1/3}(K_1 + \eta - K_3\eta^2)^{-1/3}\, d\eta}{\int_0^{1} \eta^{1/3}(K_1 + \eta - K_3\eta^2)^{-1/3}\, d\eta} \\ &\xi_1 \leq \xi \leq 1 , && \eta = 1 \end{aligned} \tag{32}$$

where ξ_0 and ξ_1 denote the abscissas of the two possible transition points. Bodies of class I can be obtained from bodies of class IV by means of the formal substitution $\xi_0 = 0$, $\xi_1 = 1$. An analogous remark holds for bodies of class II where $\xi_1 = 1$ and for bodies of class III where $\xi_0 = 0$. It should be noted, however, that the corner conditions need not be satisfied at these special points. In a functional form, Eqs. (32) can be rewritten as

$$\eta = \eta(\xi, \xi_0, \xi_1, K_1, K_3) \tag{33}$$

so that, after this equation is combined with any one of the following sets of relations:

$$\begin{aligned} &\text{Class I:} && \xi_0 = 0, && \xi_1 = 1 \\ &\text{Class II:} && K_1 = 0, && \xi_1 = 1 \\ &\text{Class III:} && \xi_0 = 0, && K_1 + 1 - K_3 = 0 \\ &\text{Class IV:} && K_1 = 0, && K_3 = 1 \end{aligned} \tag{34}$$

it is seen that a two parameter family of optimum bodies exists.

For particular types of boundary conditions, considerable simplifications are possible. Thus, if the length is free ($K_1 = 0$) or the volume is free ($K_3 = 0$), the number of independent parameters is reduced by one. An analogous remark holds for the case where the diameter is free, since $K_1 + 1 = K_3$. In conclusion, the number of independent parameters governing the solution depends on the number of geometric quantities other than the

wetted area which are prescribed. If three quantities are prescribed, the problem admits a two-parameter family of solutions. If two quantities are prescribed, the problem admits a one-parameter family of solutions. Finally, if only one quantity is prescribed, the problem admits a zero-parameter family of solutions, that is, the geometry of the extremal arc in the $\xi\eta$-plane consists of a single curve regardless of the value of the friction coefficient. In this connection, the dimensionless boundary conditions are indicated in Table 2 along with the dimensionless switching function at the final point, the slope of the extremal arc at the final point, and the number of independent parameters governing the solution.

5. SOLUTION OF THE BOUNDARY VALUE PROBLEM

In this section, a general method for determining the unknowns appearing in Eqs. (32) is presented. The analysis is facilitated if several nondimensional integrals are introduced. After the cubic root of both sides of Eq. (23) is extracted, the variables are separated, and an integration over the regular shape is performed, the following result is obtained:

$$\frac{\sqrt[3]{2C_f}}{\tau} = I_d(\xi_o, \xi_1, K_1, K_3) \tag{35}$$

where

$$\tau = d/\ell \tag{36}$$

denotes the thickness ratio and I_d the nondimensional integral

$$I_d(\xi_o, \xi_1, K_1, K_3) = \frac{1}{\xi_1 - \xi_o} \int_0^1 \eta^{1/3}(K_1 + \eta - K_3\eta^2)^{-1/3}\, d\eta \tag{37}$$

Furthermore, by simple manipulations, the wetted area and the volume can be expressed as

$$\begin{aligned} S\tau/\pi d^2 &= I_S(\xi_o, \xi_1, K_1, K_3) \\ 4V\tau/\pi d^3 &= I_V(\xi_o, \xi_1, K_1, K_3) \end{aligned} \tag{38}$$

where

$$I_S(\xi_o, \xi_1, K_1, K_3) = \int_0^1 \eta d\xi = 1 - \xi_1 + (\xi_1 - \xi_o) \frac{\int_0^1 \eta^{4/3}(K_1 + \eta - K_3\eta^2)^{-1/3}\, d\eta}{\int_0^1 \eta^{1/3}(K_1 + \eta - K_3\eta^2)^{-1/3}\, d\eta} \tag{39}$$

$$I_V(\xi_o, \xi_1, K_1, K_3) = \int_0^1 \eta^2 d\xi = 1 - \xi_1 + (\xi_1 - \xi_o) \frac{\int_0^1 \eta^{7/3}(K_1 + \eta - K_3\eta^2)^{-1/3}\, d\eta}{\int_0^1 \eta^{1/3}(K_1 + \eta - K_3\eta^2)^{-1/3}\, d\eta}$$

For a given friction coefficient, the system composed of the six equations (34) through (36) and (38) involves the nine quantities

$$\tau,\ d,\ \ell,\ S,\ V,\ \xi_o,\ \xi_1,\ K_1,\ K_3 \tag{40}$$

which means that one particular optimum body can be determined if three additional relationships are specified. For the boundary conditions considered in Table 2, these relationships are represented by any one of the following sets:

$$\begin{aligned}
&d = \text{Const}, && K_1 = 0, && K_3 = 0\\
&V = \text{Const}, && K_1 = 0, && K_3 = 1\\
&d = \text{Const}, && \ell = \text{Const}, && K_3 = 0\\
&d = \text{Const}, && V = \text{Const}, && K_1 = 0\\
&\ell = \text{Const}, && V = \text{Const}, && K_3 = K_1 + 1\\
&d = \text{Const}, && \ell = \text{Const}, && V = \text{Const}
\end{aligned} \tag{41}$$

Drag coefficient. After the boundary value problem has been solved, the next step is to determine the drag of the optimum body. This drag can be written as

$$D = \frac{\pi q d^4}{4\ell^2}\left(I_{Dp} + \frac{4C_f \ell^3}{d^3} I_S\right) \tag{42}$$

where I_{Dp} denotes the dimensionless integral

$$I_{Dp} = \int_0^1 \eta\eta'^3 d\xi \tag{43}$$

Now, if the drag coefficient is referred to the frontal area at $x = \ell$ (that is, if $C_D = 4D/\pi q d^2$), the following relationship can be readily established between the drag coefficient, the friction coefficient, and the thickness ratio:

$$\frac{C_D}{\tau^2} = I_{Dp} + 4\frac{C_f}{\tau^3} I_S \tag{44}$$

Notice that, if both sides of Eq. (23) are multiplied by $d\xi$ and integrated over the entire length of the extremal arc, the relationship

$$\frac{\tau^3}{2C_f} I_{Dp} = K_1 + I_S - \lambda_3 I_V \tag{45}$$

can be established. Consequently, after Eqs. (35), (44), and (45) are combined, one deduces that

$$\frac{C_D}{\tau^2} = I_d^3 (K_1 + 3I_S - K_3 I_V) \tag{46}$$

Drag ratio. Another interesting characteristic of the optimum body is the drag ratio, that is, the ratio of the friction drag to the total drag. Because of Eq. (44), this quantity is given by

$$\frac{C_{Df}}{C_D} = \frac{4C_f I_S}{4C_f I_S + \tau^3 I_{Dp}} \tag{47}$$

which, in the light of Eq. (45), can be rewritten as

$$\frac{C_{Df}}{C_D} = \frac{2I_S}{K_1 + 3I_S - K_3 I_V} \tag{48}$$

6. PARTICULAR CASES

In the previous sections, the minimum drag problem was solved functionally for arbitrary boundary conditions. Here, several particular cases are considered, and the associated optimum shapes are calculated. Three classes of problems are considered: (a) problems in which only one geometric quantity is prescribed, (b) problems where two geometric quantities are prescribed, and (c) problems where three geometric quantities are prescribed. At the onset, a basic lemma relative to problems with the length unspecified must be stated: Since the drag of a spike is zero regardless of its length, one can take any extremal arc of class I and generate from it an infinite number of equal drag solutions of class II by adding a spike of arbitrary length in front. Analogously, one can take any extremal arc of class III and generate from it an infinite number of equal drag solutions of class IV by adding a spike of arbitrary length in front. Because of this, whenever the length is free, only solutions of class I and/or class III are considered.

6.1. Given Diameter

If the diameter is given while the length and the volume are free, the transversality condition leads to $K_1 = K_3 = 0$. Since Eqs. (34-3) and (34-4) are not satisfied, there exists no extremal arc belonging to either class III or class IV. Furthermore, since the length is free, the basic lemma applies: one may disregard all equal drag solutions of class II and search for a basic extremal of class I, that is, involving a regular shape only.

For $\xi_0 = 0$ and $\xi_1 = 1$, the equation of the regular shape (32-2) can be integrated to yield

$$\eta = \xi \tag{49}$$

which means that the optimum body is a cone. Since $I_d = 1$, the following value is obtained from Eq. (35) for the optimum thickness ratio:

$$\tau = \sqrt[3]{2C_f} = 1.26\sqrt[3]{C_f} \tag{50}$$

Furthermore, since $I_S = 1/2$, Eq. (46) indicates that the drag coefficient per unit thickness ratio squared is given by

$$\frac{C_D}{\tau^2} = \frac{3}{2} = 1.5 \tag{51}$$

and Eq. (48) implies that the friction drag of the optimum body is two-thirds of the total drag.

6.2. Given Volume

If the volume is given while the diameter and the length are free, the transversality condition leads to $K_1 = 0$, $K_3 = 1$, and $\sigma_f = 0$. Should the zero-slope shape $\eta = 1$ exist, the switching function would be zero at both ends of this subarc. However, because of Eq. (28), this is only possible when $\xi_f = \xi_c$. Since the length of the zero-slope shape $\eta = 1$ is zero, there exists no extremal arc belonging to either class III or class IV. Furthermore, since the overall length of the body is free, the basic lemma applies: one may disregard all equal drag solutions of class II and search for a basic extremal of class I, that is, one involving a regular shape only.

This unique extremal of class I can be found by substituting $\xi_0 = 0$ and $\xi_1 = 1$ into Eq. (32-2) so that, upon integration, the equation of the regular shape becomes (Fig. 1)

$$\eta = 1 - (1 - \xi)^{3/2} \tag{52}$$

Since $I_d = 3/2$, Eq. (35) yields the following value for the optimum thickness ratio:

$$\tau = \frac{2}{3}\sqrt[3]{2C_f} = 0.84\sqrt[3]{C_f} \tag{53}$$

Finally, since $I_s = 3/5$ and $I_v = 9/20$, Eq. (46) yields the following minimum drag coefficient:

$$\frac{C_D}{\tau^2} = \frac{729}{160} = 4.56 \tag{54}$$

and Eq. (48) implies that the friction drag of the optimum body is eight-ninths of the total drag.

6.3. Given Diameter and Length

If the diameter and the length are prescribed while the volume is free, the transversality condition leads to $K_3 = 0$. Extremal solutions of class IV do not exist because Eq. (34-4) is violated. Analogously, extremal solutions of class III must be ruled out since Eq. (34-3) is solved by $K_1 = -1$ and this is incompatible with Ineq. (25-1). In conclusion, the totality of ex-

tremal arcs is represented by a one-parameter family of solutions of either class I (regular shape) or class II (spike followed by a regular shape) depending on whether the friction coefficient is smaller or larger than a certain critical value. The representation of the results is facilitated by introducing the friction parameter

$$K_f = \frac{\sqrt[3]{2C_f}}{\tau} \tag{55}$$

which, because of Eq. (35) as well as the condition that $\xi_1 = 1$, can be rewritten as

$$K_f = I_d(\xi_o, K_1) \tag{56}$$

Bodies of class I. These solutions, which were originally studied by Kennet (Ref. 3), consist of a regular shape only and are obtained for $\xi_o = 0$ and $\infty \geq K_1 \geq 0$. After Eq. (32-2) is employed, the equation of the optimum shape can be written as

$$\xi = \frac{f(\eta, K_1)}{f(1, K_1)} \tag{57}$$

where

$$f(\eta, K_1) = \sqrt[3]{\eta(K_1 + \eta)^2} + \frac{K_1}{2} \log \frac{\sqrt[3]{K_1 + \eta} - \sqrt[3]{\eta}}{\sqrt[3]{K_1}} - \frac{K_1}{\sqrt{3}} \arctan \frac{\sqrt{3}\sqrt[3]{\eta}}{\sqrt[3]{\eta} + 2\sqrt[3]{K_1 + \eta}} \tag{58}$$

Furthermore, because of Eqs. (46) and (56), the drag coefficient and the friction parameter become

$$\frac{C_D}{\tau^2} = \left[\frac{3}{2} (1 + K_1)^{2/3} - K_1 f(1, K_1) \right] f^2(1, K_1)$$

$$K_f = f(1, K_1) \tag{59}$$

Elimination of the parameter K_1 from these equations yields the functional relationships

$$\eta = \eta(\xi, K_f) , \quad \frac{C_D}{\tau^2} = \frac{C_D}{\tau^2} (K_f) \tag{60}$$

which are presented in Figs. 2 and 3 and are valid in the interval $0 \le K_f \le 1$. Incidentally, the solution corresponding to $K_f = 0$ is a 3/4-power body while the solution corresponding to $K_f = 1$ is a cone.

Bodies of class II. These solutions consist of a spike followed by a regular shape and are obtained for $0 \le \xi_0 \le 1$ and $K_1 = 0$. After the shape of the optimum body, the drag coefficient, and the friction parameter are written as

$$\begin{cases} 0 \le \xi \le \xi_0 , & \eta = 0 \\ \xi_0 \le \xi \le 1 , & \eta = \dfrac{\xi - \xi_0}{1 - \xi_0} \end{cases}$$

$$\frac{C_D}{\tau^2} = \frac{3}{2(1 - \xi_0)^2} , \quad K_f = \frac{1}{1 - \xi_0} \tag{61}$$

elimination of the abscissa of the transition point from these equations leads to functional relationships of the form (60) which are plotted in Figs. 2 and 3 and are valid for $1 \leq K_f \leq \infty$. It is worth noting that these solutions consist of spikes followed by cones with the transition point moving backwards as the friction parameter increases.

6.4. Given Diameter and Volume

If the diameter and the volume are given while the length is free, the transversality condition leads to $K_1 = 0$. Since the length is free, the fundamental lemma indicates that one should disregard all equal drag solutions of class II and class IV and search for the one-parameter family of extremal solutions of class I and class III only. These solutions occur when the friction coefficient is smaller or larger than a certain critical value, respectively. The representation of the results is facilitated by introducing the thickness and friction parameters

$$K_\tau = \frac{4V}{\pi d^3}\,\tau\,, \qquad K_f = \frac{4V}{\pi d^3}\,\sqrt[3]{2C_f} \tag{62}$$

which, because of Eqs. (35) and (38-2) as well as the condition that $\xi_0 = 0$, can be rewritten as

$$K_\tau = I_V(\xi_1, K_3)\,, \qquad K_f = I_d(\xi_1, K_3)\, I_V(\xi_1, K_3) \tag{63}$$

Bodies of class I. These bodies consist of a regular shape only and are obtained for $\xi_1 = 1$ and $-\infty \leq K_3 \leq 1$. After Eqs. (32-2), (46), and (63)

are employed, the optimum shape, the thickness parameter, the drag coefficient, and the friction parameter can be rewritten as

$$\xi = \frac{1 - (1 - K_3\eta)^{2/3}}{1 - (1 - K_3)^{2/3}}$$

$$K_\tau = \frac{1}{20K_3^2}\left[\frac{9 - (5K_3^2 + 6K_3 + 9)\,(1 - K_3)^{2/3}}{1 - (1 - K_3)^{2/3}}\right] \tag{64}$$

$$\frac{C_D}{\tau^2} = \frac{27}{160K_3^4}\left[1 - (1 - K_3)^{2/3}\right]^2\left[27 + (5K_3^2 - 18K_3 - 27)\,(1 - K_3)^{2/3}\right]$$

$$K_f = \frac{3}{40K_3^3}\left[9 - (5K_3^2 + 6K_3 + 9)\,(1 - K_3)^{2/3}\right]$$

Elimination of the parameter K_3 from these equations yields the functional relationships

$$\eta = \eta(\xi, K_f)\ , \quad K_\tau = K_\tau(K_f)\ , \quad \frac{C_D}{\tau^2} = \frac{C_D}{\tau^2}(K_f) \tag{65}$$

which are plotted in Figs. 4 through 6 and are valid in the interval $0 \le K_f \le 27/40$. Incidentally, the solution corresponding to $K_f = 0$ is a 3/2-power body, that corresponding to $K_f = 1/3$ is a cone, and that corresponding to $K_f = 27/40$ is such that the complements of the abscissa and the ordinate obey a 3/2-power law.

Bodies of class III. These solutions consist of a regular shape followed by a cylinder and are obtained for $0 \leq \xi_1 \leq 1$ and $K_3 = 1$. After the shape of the optimum body, the thickness parameter, the drag coefficient, and the friction parameter are written as

$$\begin{cases} 0 \leq \xi \leq \xi_1 , & \eta = 1 - \left(1 - \dfrac{\xi}{\xi_1}\right)^{3/2} \\ \xi_1 \leq \xi \leq 1 , & \eta = 1 \end{cases}$$

$$K_\tau = 1 - \frac{11}{20}\,\xi_1 \tag{66}$$

$$\frac{C_D}{\tau^2} = \left(\frac{3}{2\xi_1}\right)^3 \left(2 - \frac{13}{20}\,\xi_1\right)$$

$$K_f = \frac{3}{2\xi_1}\left(1 - \frac{11}{20}\,\xi_1\right)$$

elimination of the abscissa of the transition point leads to functional relationships of the form (65) which are plotted in Figs. 4 through 6 and are valid in the interval $27/40 \leq K_f \leq \infty$. In closing, it is worth noting that the transition point shifts forward as the friction parameter increases.

6.5. Given Length and Volume

If the length and the volume are given while the diameter is free, the transversality condition leads to $K_3 = K_1 + 1$ and $\sigma_f = 0$. Should the zero-slope shape $\eta = 1$ exist, the switching function would be zero at both ends of this subarc, and this would imply that $\xi_f = \xi_c$. Since the length of the zero-slope shape $\eta = 1$ is zero, there exists no extremal arc belonging to

either class III or class IV. Consequently, the totality of extremal arcs is represented by a one-parameter family of solutions of either class I (regular shape) or class II (spike followed by a regular shape) depending on whether the friction coefficient is smaller or larger than a certain critical value. The representation of the results is facilitated if a thickness parameter and a friction parameter are introduced. These parameters are defined by

$$K_\tau = \sqrt{\frac{\pi \ell^3}{4V}}\,\tau\,, \qquad K_f = \sqrt{\frac{\pi \ell^3}{4V}}\,\beta\overline{2C_f} \tag{67}$$

and, because of Eqs. (35) and (38-2) as well as the condition that $\xi_1 = 1$, can be rewritten as

$$K_\tau = I_V^{-1/2}(\xi_o, K_1)\,, \qquad K_f = I_d(\xi_o, K_1) I_V^{-1/2}(\xi_o, K_1) \tag{68}$$

Bodies of class I. These solutions consist of a regular shape only and are obtained for $\xi_o = 0$ and $\infty \geq K_1 \geq 0$. If Eq. (32-2) is employed, the optimum shape can be rewritten as

$$\xi = \frac{g(\eta, K_1)}{g(1, K_1)} \tag{69}$$

where

$$g(\eta, K_1) = \int_0^\eta \eta^{1/3} \left[K_1 + \eta - (1 + K_1)\,\eta^2\right]^{-1/3} d\eta \tag{70}$$

Furthermore, Eqs. (46) and (68) yield the following expressions for the thickness parameter, the drag coefficient, and the friction parameter:

$$K_\tau = \sqrt{\frac{g(1, K_1)}{h(K_1)}}$$

$$\frac{C_D}{\tau^2} = g^2(1, K_1)\left[K_1\, g(1, K_1) - (1 + K_1)\, h(K_1) + 3i(K_1)\right] \qquad (71)$$

$$K_f = \sqrt{\frac{g^3(1, K_1)}{h(K_1)}}$$

where

$$h(K_1) = \int_0^1 \eta^{7/3}\left[K_1 + \eta - (1 + K_1)\,\eta^2\right]^{-1/3} d\eta$$

$$i(K_1) = \int_0^1 \eta^{4/3}\left[K_1 + \eta - (1 + K_1)\,\eta^2\right]^{-1/3} d\eta \qquad (72)$$

Elimination of the parameter K_1 from Eqs. (69) and (71) yields functional relationships of the form (65) which are presented in Figs. 7 through 9 and are valid in the interval $0 \le K_f \le \sqrt{5}$.

Bodies of class II. These solutions consist of a spike followed by a regular shape and are obtained for $0 \le \xi_0 \le 1$ and $K_1 = 0$. After the shape of the optimum body, the thickness parameter, the drag coefficient, and the friction parameter are written as

$$\begin{cases} 0 \le \xi \le \xi_0 , & \eta = 0 \\ \xi_0 \le \xi \le 1 , & \eta = 1 - \left(\frac{1-\xi}{1-\xi_0}\right)^{3/2} \end{cases}$$

$$K_\tau = \frac{2\sqrt{5}}{3(1-\xi_0)^{1/2}} \qquad (73)$$

$$\frac{C_D}{\tau^2} = \frac{2}{5}\left(\frac{3}{2}\right)^6 \frac{1}{(1-\xi_0)^2}$$

$$K_f = \frac{\sqrt{5}}{(1-\xi_0)^{3/2}}$$

elimination of the abscissa of the transition point leads to functional relationships of the form (65) which are plotted in Figs. 7 through 9 and are valid in the interval $\sqrt{5} \le K_f \le \infty$. Notice that, as the friction parameter increases, the transition point moves backward.

6.6. Given Diameter, Length, and Volume

If the diameter, the length, and the volume are given while the wetted area is free, a two-parameter family of solutions exists and includes bodies belonging to each of the four classes defined previously. The representation of the results is facilitated if one defines the shape parameter and the friction parameter as

$$K_s = \frac{4V_\tau}{\pi d^3} , \quad K_f = \frac{\sqrt[3]{2C_f}}{\tau} \qquad (74)$$

and observes that these parameters satisfy the conditions (35) and (38-2).

Bodies of class I. These solutions consist of a regular shape only and are obtained when conditions (34-1) are satisfied. Consequently, the shape of the optimum body is given by

$$\xi = \frac{g(\eta, K_1, K_3)}{g(1, K_1, K_3)} \tag{75}$$

where

$$g(\eta, K_1, K_3) = \int_0^{\eta} \eta^{1/3}(K_1 + \eta - K_3\eta^2)^{-1/3}\, d\eta \tag{76}$$

The associated drag coefficient, shape parameter, and friction parameter become

$$\frac{C_D}{\tau^2} = g^2(1, K_1, K_3)\left[K_1 g(1, K_1, K_3) - K_3 h(K_1, K_3) + 3i(K_1, K_3)\right]$$

$$K_s = \frac{h(K_1, K_3)}{g(1, K_1, K_3)} \tag{77}$$

$$K_f = g(1, K_1, K_3)$$

where

$$h(K_1, K_3) = \int_0^1 \eta^{7/3}\left[K_1 + 1 - K_3\eta^2\right]^{-1/3} d\eta$$

$$i(K_1, K_3) = \int_0^1 \eta^{4/3}\left[K_1 + 1 - K_3\eta^2\right]^{-1/3} d\eta \tag{78}$$

Elimination of the parameters K_1 and K_3 from Eqs. (75) and (77) yields functional relationships of the form

$$\eta = \eta(\xi, K_s, K_f) , \quad \frac{C_D}{\tau^2} = \frac{C_D}{\tau^2}(K_s, K_f) \tag{79}$$

which are plotted in Figs. 10 through 15.

Bodies of class II. These solutions consist of a spike followed by a regular shape and are obtained when conditions (34-2) are satisfied. After the shape of the optimum body, the drag coefficient, the shape parameter, and the friction parameter are written as

$$\begin{cases} 0 \le \xi \le \xi_0 , & \eta = 0 \\ \xi_0 \le \xi \le 1 , & \xi = \xi_0 + (1 - \xi_0) \dfrac{1 - (1 - K_3\eta)^{2/3}}{1 - (1 - K_3)^{2/3}} \end{cases}$$

$$\frac{C_D}{\tau^2} = \frac{2}{5}\left(\frac{3}{4}\right)^3 \left[\frac{1 - (1 - K_3)^{2/3}}{(1 - \xi_0) K_3^2}\right]^2 \left[27 + (5K_3^2 - 18K_3 - 27)(1 - K_3)^{2/3}\right] \tag{80}$$

$$K_s = \frac{1 - \xi_0}{20K_3^2\left[1 - (1 - K_3)^{2/3}\right]}\left[9 - (5K_3^2 + 6K_3 + 9)(1 - K_3)^{2/3}\right]$$

$$K_f = \frac{3}{2K_3(1 - \xi_0)}\left[1 - (1 - K_3)^{2/3}\right]$$

elimination of the parameters ξ_0 and K_3 yields functional relationships of the form (79) which are plotted in Figs. 10 through 15.

Bodies of class III. These solutions consist of a regular shape followed by a cylinder and are obtained when conditions (34-3) are satisfied. The shape of the optimum body is given by

$$\begin{cases} 0 \le \xi \le \xi_1 , & \dfrac{\xi}{\xi_1} = \dfrac{g(\eta, K_1)}{g(1, K_1)} \\ \xi_1 \le \xi \le 1 , & \eta = 1 \end{cases} \tag{81}$$

where

$$g(\eta, K_1) = \int_0^{\eta} \eta^{1/3} \left[K_1 + \eta - (1 + K_1)\eta^2\right]^{-1/3} d\eta \tag{82}$$

Furthermore, the drag coefficient, the shape parameter, and the friction parameter become

$$\frac{C_D}{\tau^2} = \frac{g^2(1, K_1)}{\xi_1^2} \left[2g(1, K_1) \frac{1 - \xi_1}{\xi_1} + K_1 g(1, K_1) - (1 + K_1)\, h(K_1) + 3i(K_1)\right]$$

$$K_s = 1 - \xi_1 + \xi_1 \frac{h(K_1)}{g(1, K_1)} \tag{83}$$

$$K_f = \frac{g(1, K_1)}{\xi_1}$$

where

$$\begin{aligned} h(K_1) &= \int_0^1 \eta^{7/3} \left[K_1 + \eta - (K_1 + 1)\eta^2\right]^{-1/3} d\eta \\ i(K_1) &= \int_0^1 \eta^{4/3} \left[K_1 + \eta - (K_1 + 1)\eta^2\right]^{-1/3} d\eta \end{aligned} \tag{84}$$

Elimination of the parameters ξ_1 and K_1 from Eqs. (81) and (83) yields functional relationships of the form (79) which are plotted in Figs. 10 through 15.

Bodies of class IV. These solutions consist of a spike followed by a regular shape followed by a cylinder and are obtained when conditions (34-4) are satisfied. After the geometry of the optimum body, the drag coefficient, the shape parameter, and the friction parameter are written as

$$\begin{cases} 0 \le \xi \le \xi_0 , & \eta = 0 \\ \xi_0 \le \xi \le \xi_1 , & \eta = 1 - \left(\dfrac{\xi_1 - \xi}{\xi_1 - \xi_0} \right)^{3/2} \\ \xi_1 \le \xi \le 1 , & \eta = 1 \end{cases} \tag{85}$$

$$\frac{C_D}{\tau^2} = \left[\frac{3}{2(\xi_1 - \xi_0)} \right]^3 \left[2 - \frac{27\xi_0 + 13\xi_1}{20} \right]$$

$$K_s = 1 - \frac{9\xi_0 + 11\xi_1}{20}$$

$$K_f = \frac{3}{2(\xi_1 - \xi_0)}$$

elimination of the parameters ξ_0 and ξ_1 leads to functional relationships of the form (79) which are plotted in Figs. 10 through 15.

Limiting curves. Now that the relationships concerning the geometry of the body, the drag coefficient, the shape parameter, and the friction parameter have been derived, it is useful to determine the shape parameter-

friction parameter region in which the equations governing each class of bodies are valid. After simple algebraic manipulations, the parametric equations defining the limiting curves between the different classes of bodies are given by

$$\text{I - II} \quad \begin{cases} K_s = \dfrac{1}{20K_3^2} \dfrac{9 - (5K_3^2 + 6K_3 + 9)(1 - K_3)^{2/3}}{1 - (1 - K_3)^{2/3}} \\ K_f = \dfrac{3}{2} \dfrac{1 - (1 - K_3)^{2/3}}{K_3} \end{cases}$$

$$\text{I - III} \quad \begin{cases} K_s = \dfrac{h(K_1)}{g(1, K_1)} \\ K_f = g(1, K_1) \end{cases} \qquad (86)$$

$$\text{II - IV} \quad \begin{cases} K_s = \dfrac{9}{20}(1 - \xi_0) \\ K_f = \dfrac{3}{2(1 - \xi_0)} \end{cases}$$

$$\text{III - IV} \quad \begin{cases} K_s = 1 - \dfrac{11}{20}\xi_1 \\ K_f = \dfrac{3}{2\xi_1} \end{cases}$$

and, if the relevant parameters are eliminated, yield the functional relation

$$K_f = K_f(K_s) \tag{87}$$

which is presented in Fig. 16. Notice that no solution of class IV exists for $K_f < 3/2$ and no solution of class I exists for $K_f > 3/2$. Furthermore, no solution of class III occurs for $K_s < 9/20$ and no solution of class II occurs for $K_s > 9/20$.

7. DISCUSSION AND CONCLUSIONS

From the previous analysis, it appears that, despite the generality of the present problem, the method of solution is relatively simple and has the merit of leading to analytical solutions in each of the particular cases considered here. The main comments to these solutions are as follows:

(a) For the general problem in which the wetted area is free and arbitrary conditions are assigned to the diameter, the length, and the volume, the totality of extremal arcs is represented by a two-parameter family of solutions if dimensionless coordinates are employed, that is, if the abscissa and the ordinate are normalized with respect to the length and the radius. Each member of the family may involve at most two corner points and, hence, three subarcs. Of these subarcs, one is characterized by a positive pressure coefficient and is called the regular shape; the other two are characterized by a zero pressure coefficient and are called zero-slope shapes. Consequently, four classes of bodies can be identified: (I) bodies composed of a regular shape only, (II) bodies composed of a spike followed by a regular shape, (III) bodies composed of a regular shape followed by a cylinder, and (IV) bodies composed of a spike followed by a regular shape followed by a cylinder.

(b) If only one geometric quantity is assigned (the diameter or the volume) a zero-parameter family of solutions exists (that is, a single curve). In all cases, the solution is of class I, that is, consists of a regular shape only. In particular, if the diameter is given, the solution is a cone whose slope is such that the friction drag is 2/3 of the total drag. On the other hand, if the volume is given, the complements of the ordinate and

the abscissa obey a 3/2-power law, and the thickness ratio of the optimum body is such that the friction drag is 8/9 of the total drag.

(c) If two geometric quantities are prescribed (the diameter and the length, the diameter and the volume, or the length and the volume), a one-parameter family of solutions exists. This parameter, called the friction parameter, is proportional to the cubic root of the friction coefficient and is indicative of the relative importance of the friction drag with respect to the pressure drag. The analysis shows that two distinct behaviors are possible depending on whether the friction parameter is subcritical (smaller than a certain critical value) or supercritical (larger than a certain critical value). If the diameter and the length or the length and the volume are given, the solution is of class I for subcritical friction parameters and class II for supercritical friction parameters with the transition point from the spike to the regular shape shifting backwards as the friction parameter increases. On the other hand, if the diameter and the volume are given, the solution is of class I for subcritical friction parameters and class III for supercritical friction parameters with the transition point from the regular shape to the cylinder shifting forward as the friction parameter increases.

(d) If three geometric quantities are prescribed (the diameter, the length, and the volume), a two-parameter family of solutions exists. These parameters, called the friction and shape parameters, determine the existence of solutions belonging to each of the four classes defined previously.

In closing, it is worth noting that, if the limiting process $C_f \to 0$ is carried out, the present solutions reduce to the inviscid flow solutions already calculated in Refs. 1 and 2. It should also be noted that some of

the optimum shapes obtained in the analysis are concave; consequently, these bodies should be restudied using the Newton-Busemann pressure coefficient law; this, however, requires a more thorough understanding of the friction drag associated with the possible presence of free layers. Finally, when the square of the thickness ratio becomes nonnegligible with respect to one, the slender body approximation is violated; consequently, this case should be reinvestigated using the exact Newtonian expression for the pressure coefficient, that is, the sine square law.

REFERENCES

1. MIELE, A., "Optimum Slender Bodies of Revolution in Newtonian Flow", Boeing Scientific Research Laboratories, Flight Sciences Laboratory, TR No. 56, 1962.

2. HULL, D. G., "On Slender Bodies of Minimum Drag in Newtonian Flow", Boeing Scientific Research Laboratories, Flight Sciences Laboratory, TR No. 67, 1963.

3. KENNET, H., "The Effect of Friction on Optimum Minimum-Drag Shapes in Hypersonic Flow", Journal of the Aerospace Sciences, Vol. 29, No. 12, 1962.

4. MIELE, A. and COLE, J., "A Study of Optimum Slender Bodies in Hypersonic Flow with a Variable Friction Coefficient", Boeing Scientific Research Laboratories, Flight Sciences Laboratory, TR No. 66, 1963.

5. MIELE, A. and PRITCHARD, R. E., "Slender, Two-Dimensional Bodies Having Minimum Total Drag at Hypersonic Speeds", Boeing Scientific Research Laboratories, Flight Sciences Laboratory, TR No. 71, 1963.

6. MIELE, A., "The Calculus of Variations in Applied Aerodynamics and Flight Mechanics", Boeing Scientific Research Laboratories, Flight Sciences Laboratory, TR No. 41, 1961.

7. MIELE, A., Editor, "Extremal Problems in Aerodynamics", Academic Press, New York (in publication).

TABLE 1

BOUNDARY CONDITIONS

Quantities given	C_1	C_2	C_3	C	$\lambda_{4f}+3y_f\dot{y}_f^2$	Additional relationships
d	-1	0	0	0		$\dot{y}_f = \sqrt[3]{C_f/4}$
V	-1	0		0	0	$\lambda_{4f} = 0\ ,\quad \dot{y}_f = 0\ ,\quad C_f = C_3 d$
d, ℓ	-1	0	0			$\dot{y}_f = \sqrt[3]{\frac{C_f}{4} + \frac{C}{d}}$
d, V	-1	0		0		$\dot{y}_f = \sqrt[3]{\frac{C_f - C_3 d}{4}}$
ℓ, V	-1	0			0	$\lambda_{4f} = 0\ ,\quad \dot{y}_f = 0\ ,\quad C = \frac{C_3 d^2 - C_f d}{4}$
d, ℓ, V	-1	0				$\dot{y}_f = \sqrt[3]{\frac{C_f - C_3 d}{4} + \frac{C}{d}}$

TABLE 2

NONDIMENSIONAL BOUNDARY CONDITIONS

Quantities given	K_1	K_3	σ_f	$\frac{\tau\dot{\eta}_f}{\sqrt[3]{2C_f}}$	Number of Independent Parameters
d	0	0		1	0
V	0	1	0	0	0
d, ℓ		0		$\sqrt[3]{K_1 + 1}$	1
d, V	0			$\sqrt[3]{1 - K_3}$	1
ℓ, V		$K_1 + 1$	0	0	1
d, ℓ, V				$\sqrt[3]{K_1 + 1 - K_3}$	2

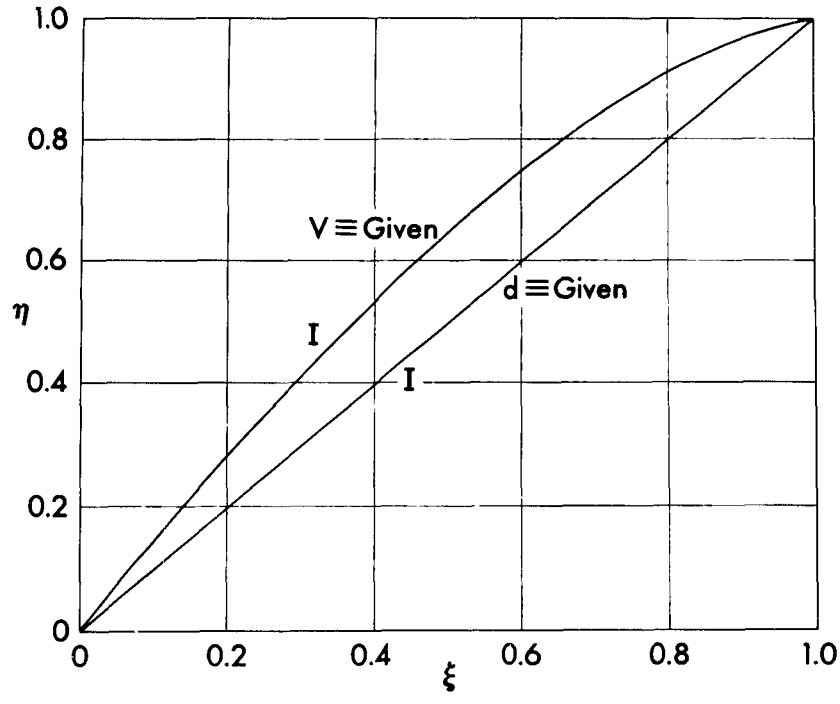

Fig. 1. Optimum shapes for given diameter and given volume.

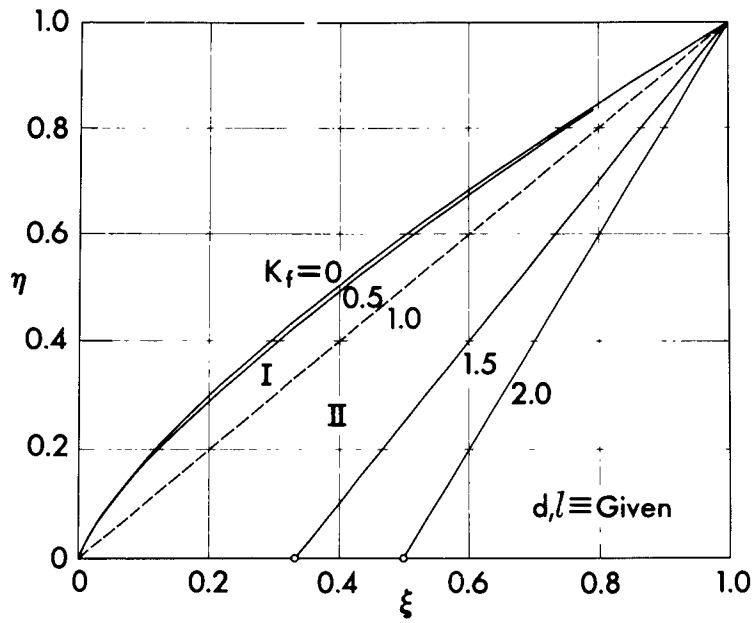

Fig. 2. Optimum shapes for given diameter and length.

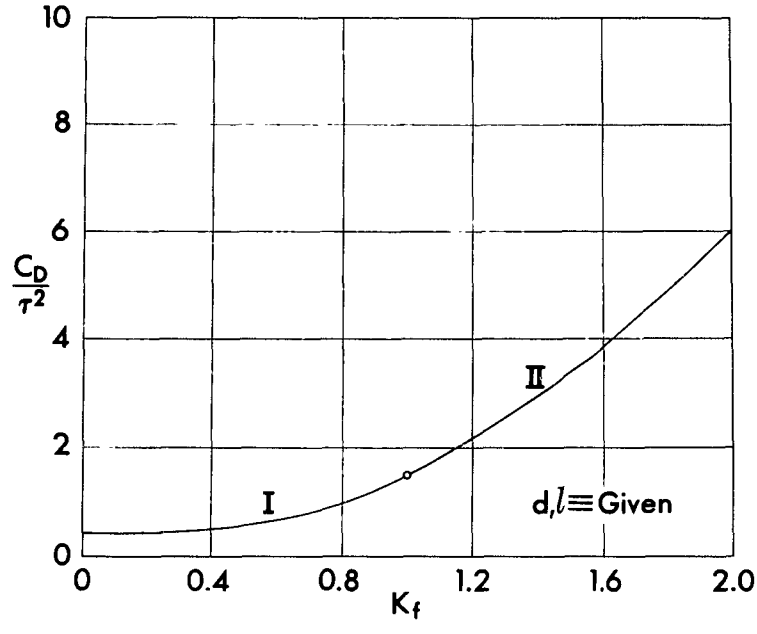

Fig. 3. Drag coefficient for given diameter and length.

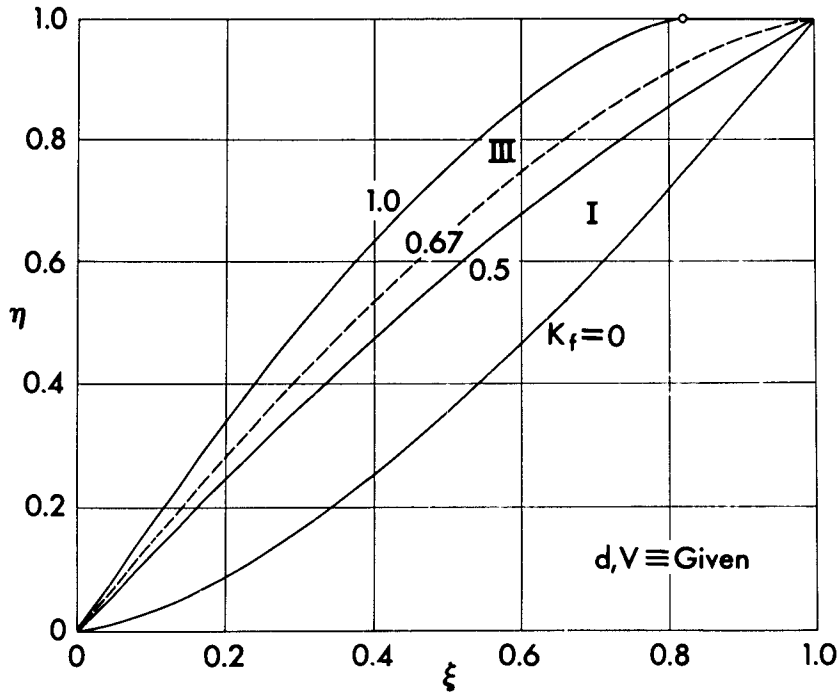

Fig. 4. Optimum shapes for given diameter and volume.

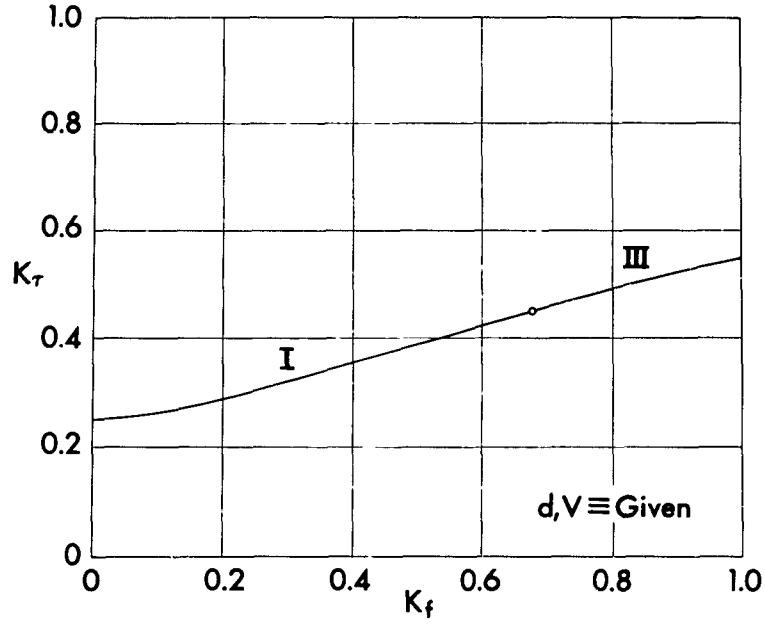

Fig. 5. Thickness parameter for given diameter and volume.

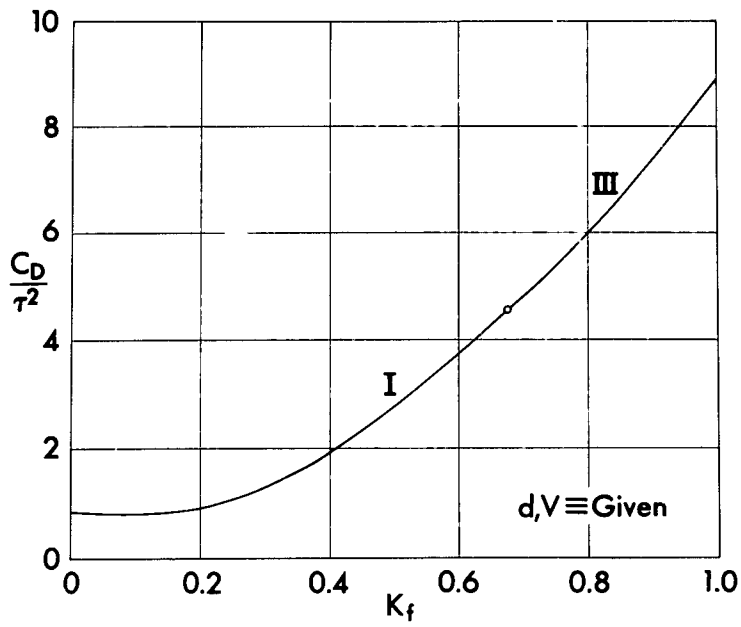

Fig. 6. Drag coefficient for given diameter and volume.

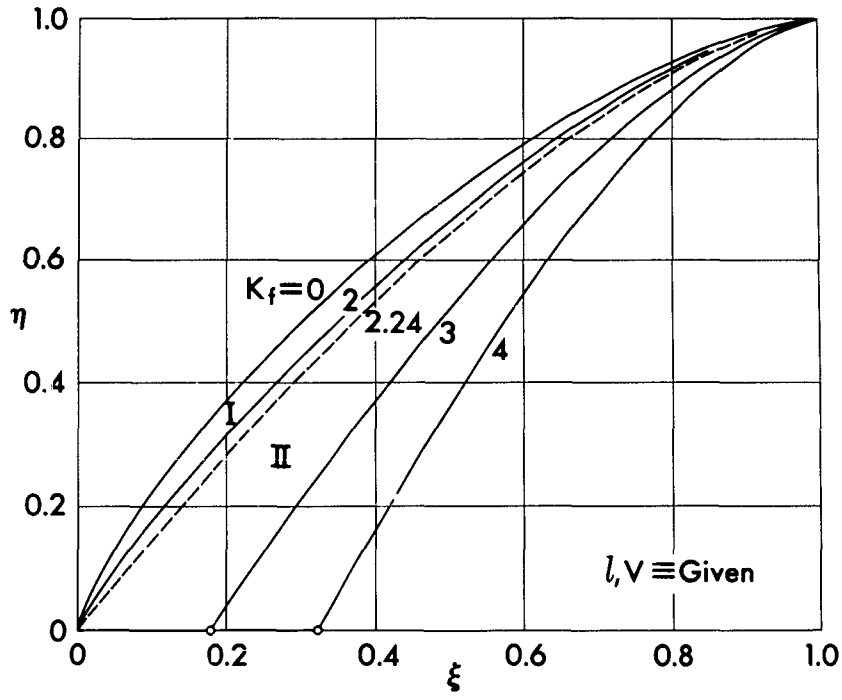

Fig. 7. Optimum shapes for given length and volume.

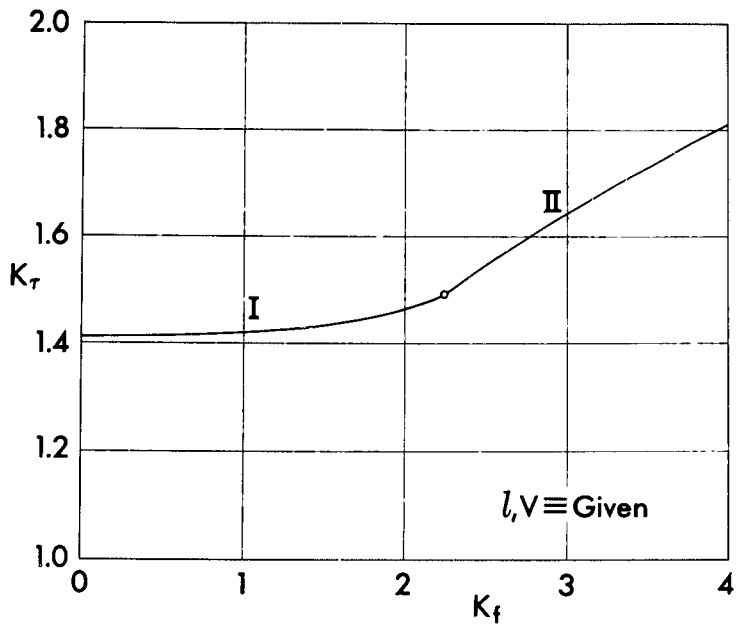

Fig. 8. Thickness parameter for given length and volume.

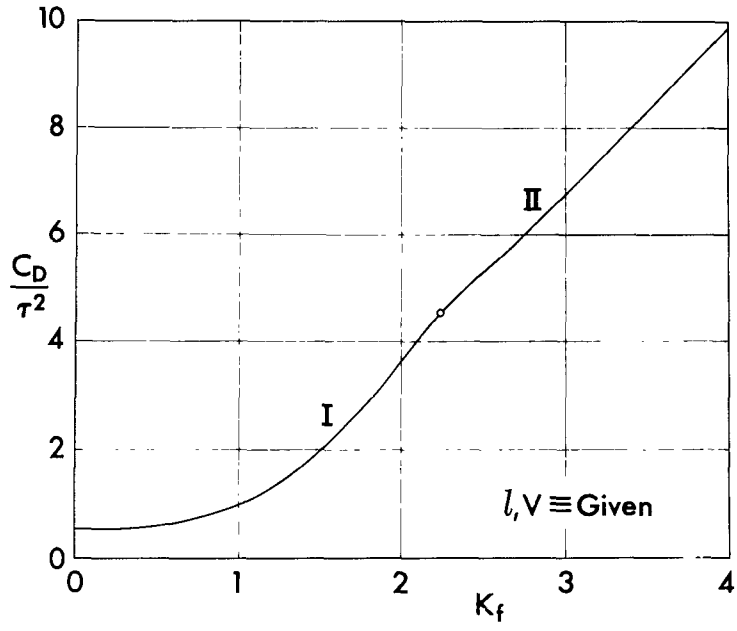

Fig. 9. Drag coefficient for given length and volume.

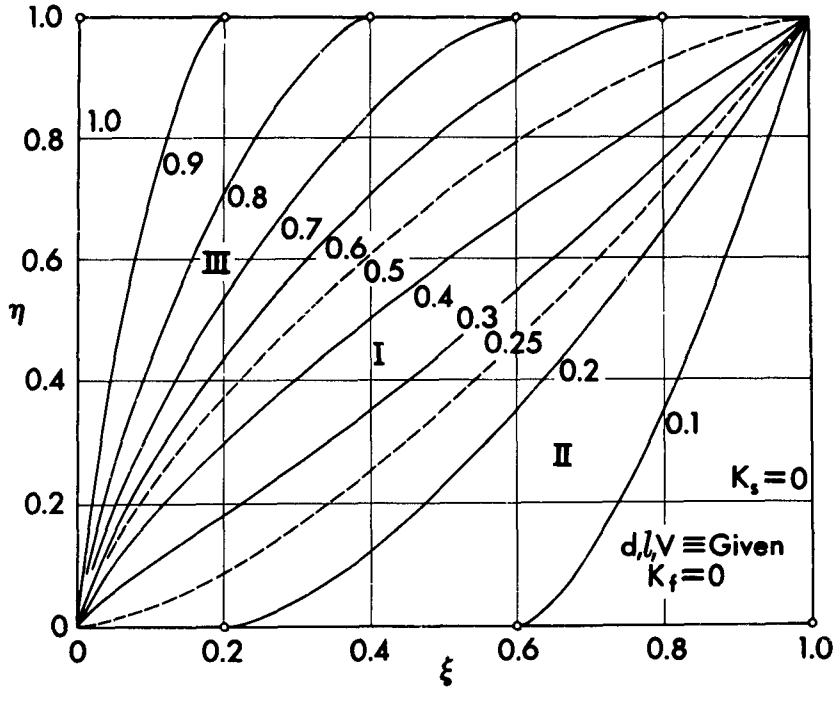

Fig. 10. Optimum shapes for given diameter, length, and volume.

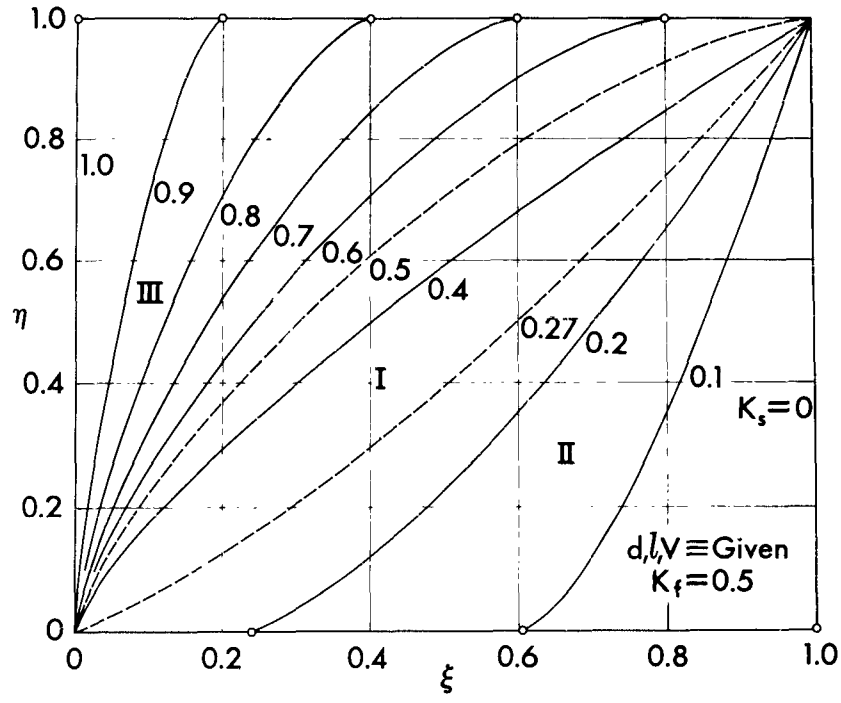

Fig. 11. Optimum shapes for given diameter, length, and volume.

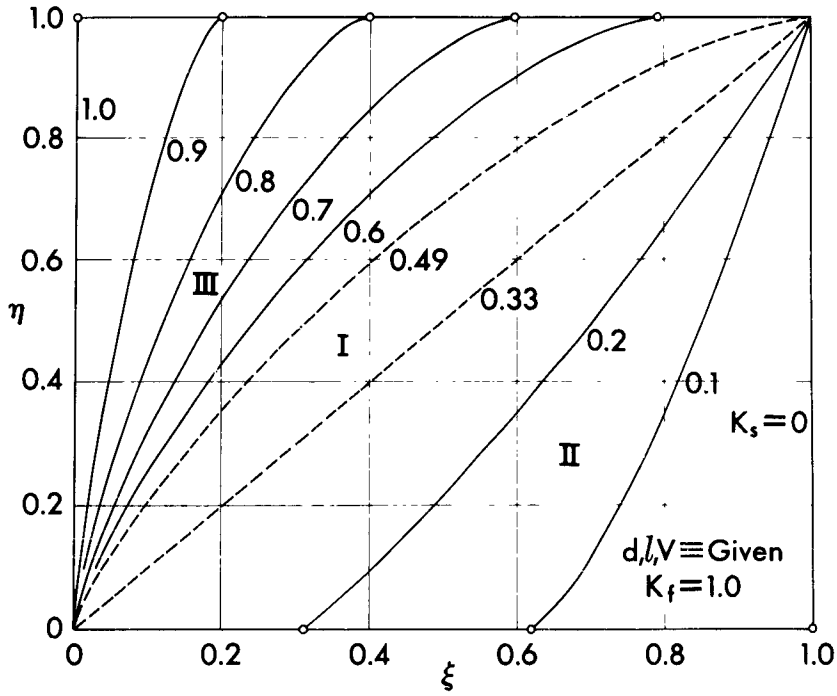

Fig. 12. Optimum shapes for given diameter, length, and volume.

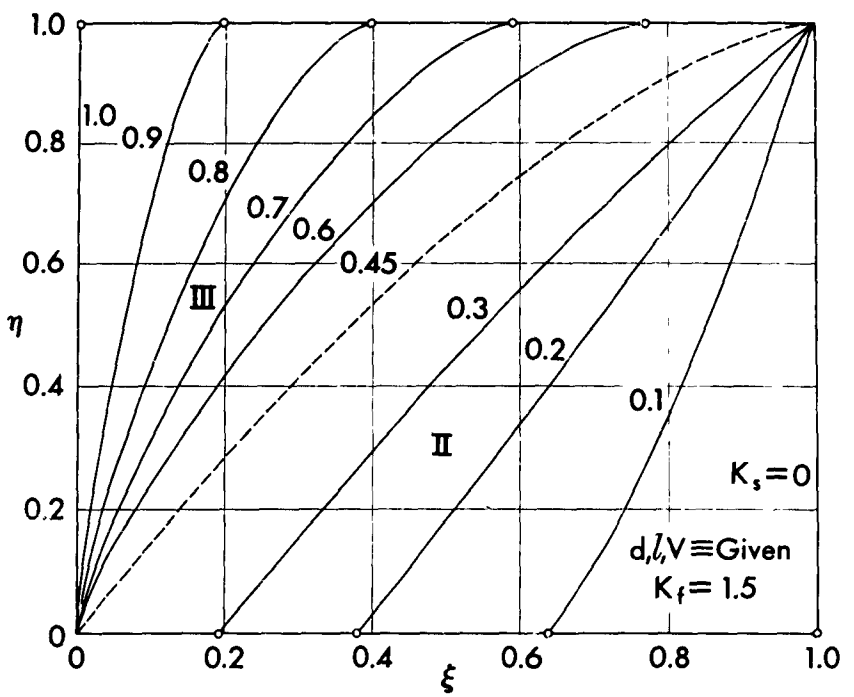

Fig. 13. Optimum shapes for given diameter, length, and volume.

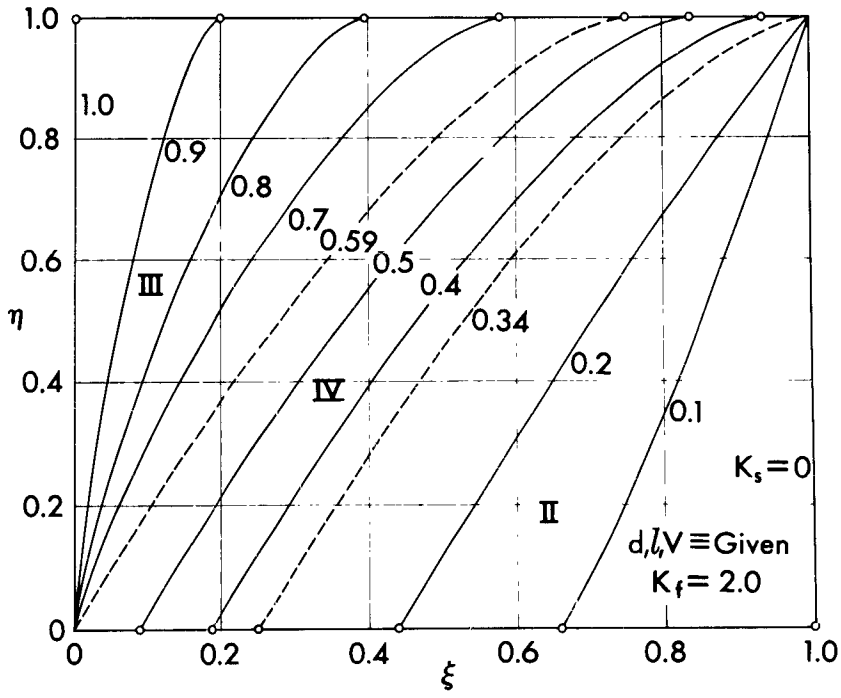

Fig. 14. Optimum shapes for given diameter, length, and volume.

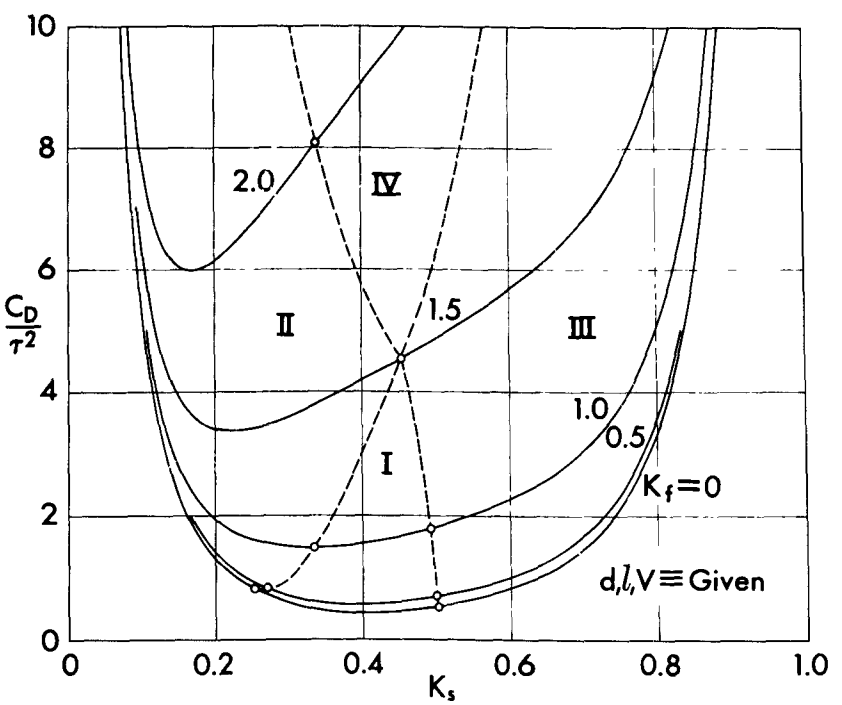

Fig. 15. Drag coefficient for given diameter, length, and volume.

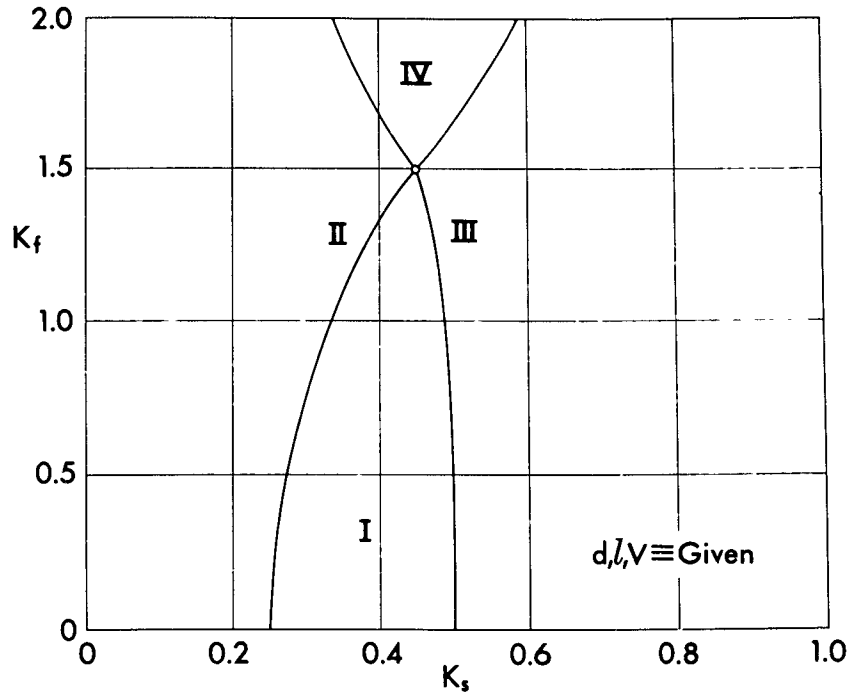

Fig. 16. Limiting curves for given diameter, length, and volume.